

Monte Carlo Analysis of Fetal Dose Distribution in Pregnancy for Different Fetal Ages, Beam Location, Beam Energy, and Field Sizes

Khusniatun Nikmah¹, Muhammad Vitro Ramadhan¹, Tony Sumaryada¹, Muhammad Fahdillah Rhani², Abd. Djamil Husin¹, Sitti Yani^{1*}

¹ Department of Physics, Faculty of Mathematics and Natural Science IPB University, Indonesia

² Department of Radiology, Kathleen Kilgour Centre, New Zealand.

Corresponding Authors E-mail: sittiyani@apps.ipb.ac.id

Article Info

Article info:

Received: 23-09-2024

Revised: 22-12-2024

Accepted: 21-01-2025

Keywords:

EGSnrc; fetal dose; Monte Carlo method; pregnancy

How To Cite:

K. Nikmah, M. V. Ramadhan, T. Sumaryada, M. F. Rhani, A. D. Husin, and S. Yani, "Monte Carlo Analysis of Fetal Dose Distribution in Pregnancy for Different Fetal Ages, Beam Location, Beam Energy, and Field Sizes", *Indonesian Physical Review*, vol. 8, no. 1, p 328-339, 2025.

DOI:

<https://doi.org/10.29303/ipr.v8i1.406>

Abstract

Treatment with radiotherapy in pregnant women may occur due to some critical conditions. The dose given during the treatment process is not only received by the patient but can also be absorbed by the fetus which can affect its growth. Moreover, the radiation target is near the fetus such as the lung. This study aims to determine the dose distribution to the fetus with variations in fetal age (trimester 1, 2, and 3), beam energy, field size, and fetal distance to the target location (lung). The entire simulation utilized the Monte Carlo-based software EGSnrc-DOSXYZnrc which produced a 3-dimensional dose distribution on the virtual phantom. The simulated virtual phantom is a box with a size of 40×40×40 cm³ containing several materials, namely water, tissue, and lung. The size of the fetus is varied according to trimesters 1, 2, and 3. The beam is in the form of monoenergetic photons with energies of 3 MeV and 5 MeV emitted from above with a source to surface distance (SSD) of 48 cm. The field size was set at 5×5 cm² and 8×8 cm² on the phantom surface. The beam axis was located at a distance of 5 cm and 3 cm from the fetus. The results showed that the four variations performed affected the fetal dose, where the fetal dose increased considerably when the field size was enlarged and the beam axis was closer to the fetal position. The increase in fetal dose is also influenced by the increase in fetal age and beam energy. Meanwhile, the location of the beam below the lung causes an increased dose to the fetus due to the closer position of the beam to the fetus.



Copyright (c) 2025 by Author(s). This work is licensed under a Creative Commons Attribution-ShareAlike 4.0 International License.

Introduction

In 2020, lung cancer is one of the leading causes of death, accounting for 13.2% (30,843 deaths) in Indonesia [1]. Lung cancer did not have specific symptoms, making it difficult to diagnose [2-25]. Lung cancer treatment could be done using surgery, radiation therapy, chemotherapy, targeted therapy, and immunotherapy. Lung cancer radiotherapy works by controlling the growth of cancer cells [3-6]. Radiotherapy could adjust the target shape and reduce risks to

healthy tissue. However, radiotherapy could cause physiological and genetic risks [7]. These risks were particularly concerning for pregnant patients. The potential impacts of radiotherapy included miscarriage, premature birth, and death [8-11]. Thus, it was essential to understand the radiation dose distribution to the fetus.

Monte Carlo (MC) is commonly used to calculate dose in complex geometries, including fetal dose distributions [12-14]. MC is a powerful and commonly used tool to simulate particle transport and calculate the energy deposited in a given volume in homogeneous and inhomogeneous materials [15-17]. Monte Carlo (MC) is considered the “gold standard” for dose calculations and particle transport in radiotherapy, which can precisely calculate doses in complicated geometries and inhomogeneous material such as human tissue [18-20]. Some MC codes that are widely used in radiotherapy are *EGSnrc* [16-17], *MCNP*, *PHITS*, and *PENELOPE* [21]. *EGSnrc* is a widely used software for simulating electron and positron photons developed by the National Research Council of Canada that can also be used to simulate fetal dose distribution.

Research on dose distribution in fetal has been conducted by Benameur et al. (2023). They used the Monte Carlo code GATE to estimate the fetal radiation dose for a pregnant patient treated for Hodgkin's lymphoma. The pregnant patient was modeled with a voxelized pregnant female phantom with gestational age at week 24. The results of this study showed that the average absorbed fetal dose was 26.18 *mGy* [22]. Another study has been conducted by simulating fetal radiation dose distribution in pregnant women with breast cancer. The beam used was an X-ray with an energy of 6 MV. The gestational age (fetus) was set in the first and second trimesters with a phantom size of 30×30×5 cm³. The study concluded that the fetus received a maximum radiation dose of 22 *mGy* and 70 *mGy* in the first and second trimesters, respectively [13]. Geng et al. (2016) used Monte Carlo TOPAS to evaluate the scattered photon dose, secondary neutron dose, and equivalent dose received by a sensitive fetus from photon and proton radiotherapy when treating brain tumors during pregnancy using an anthropomorphic pregnancy phantom with three stages (3, 6, 9 months). The results obtained show that pregnant women with brain tumors can be treated with pencil beam scans that pose no risk to the fetus [23].

This study aimed to simulate radiation dose distribution to the fetus using Monte Carlo (MC) simulation. A dose distribution simulation was performed on lung cancer of pregnant women with varied gestational (fetal) ages.

Experimental Method

The simulation was conducted using the Monte Carlo method with *EGSnrc* software. *EGSnrc* was developed explicitly for *linac* modeling and dose calculations [24]. This simulation used *isource* = 3 or Point Source Rectangular Beam Incident from the Front. The source used was a photon beam with energies of 3 MeV and 5 MeV. The beams were emitted from the front at a distance of 48 cm (Source to Surface Distance = 48 cm). The phantom was illustrated as a box with dimensions of 40×40×40 cm³. The materials used in the phantom included bone, fetus, water, and lung. The bone and lung are at a depth of 2 and 4 cm from the surface of the phantom, respectively (the distance between the bone and lung is 2 cm). The dimensions of the lung are 8×8×8 cm³. The following is the simulation setup that was conducted [23].

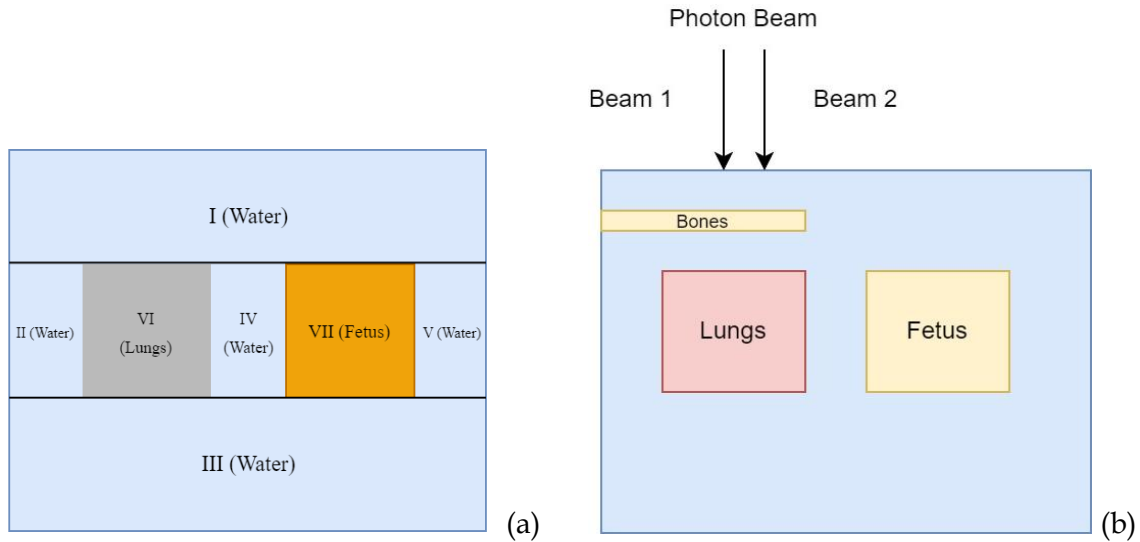


Figure 1. Phantom illustration (a) top view (b) side view

The phantom was illustrated in Figure 1. The lung and fetus were located at a depth of 4 cm from the surface. The field size was set to sizes of 5×5 cm² and 8×8 cm². There were two irradiation locations, namely irradiation 1 and irradiation 2. Irradiation 1 was 5 cm away from the fetus or right in the middle of the lung, while irradiation 2 was set 3 cm away from the fetus or in the lower part of the lung. The simulation involved 100 million particles. The phantom illustrating the fetus varied according to the trimester. The fetus was set at trimester 1, trimester 2, and trimester 3. The volume of the fetus in the first trimester was 128 cm³ with a distance of 3 cm between the lung and the fetus. In the second trimester, the volume of the fetus was 512 cm³ with a distance of 2 cm between the lung and the fetus. In the third trimester, the volume of the fetus reached 1.152 cm³ with a distance of 1 cm between the lung and the fetus. Fetal size in each trimester was obtained from Utami et al. 2020 [29].

Data analysis was conducted using the outputs from *DOSXYZnrc*, specifically the *.3ddose* and *.egsphant* files. These files were then analyzed using MATLAB to obtain isodose and DVH curves. Isodose curves were used to observe the dose distribution received by the cancer and surrounding organs [12, 25]. DVH curves in radiotherapy simulation provided a 3D visualization of the received dose [8].

Results and Discussion

Implementation of radiotherapy for pregnant women requires careful consideration to provide the best care for both the mother and the fetus. The radiation dose received by the fetus had to be minimized. In this study, a pregnant woman with lung cancer was irradiated using photon beams while varying the irradiation location (distance between the fetus and the irradiation site), fetal age, photon beam energy, and field size. The results were presented as isodose and Dose Volume Histogram (DVH) curves.

Isodose curves were used to observe the dose distribution received by cancerous and surrounding healthy tissues. These curves were derived from *.3ddose* and *.egsphant* files and were analyzed using MATLAB-based VDOSE. The DVH curve represents the dose

distribution tissues or organs receive in 3D. The x -axis on the DVH curve shows the percentage of the dose received, while the y -axis shows the percentage of the volume receiving the dose [21].

Fetal Age

The fetus's age varied based on the trimester. The fetus in the first trimester was estimated to be 3 months old, the second trimester was 6 months old, and the third trimester was 9 months old. The simulation was conducted using 5 MeV photon beams, with a field size of $8 \times 8 \text{ cm}^2$, and the irradiation location at irradiation 2 was set 3 cm away from the fetus. The isodose curves were extracted at a depth of 4 cm or slice 21. Figures 4 and 5, respectively, showed the isodose and DVH curves for the variation in fetal age. The volume of the fetus in the first trimester was 128 cm^3 , in the second trimester was 512 cm^3 , and in the third trimester was 1.152 cm^3 .

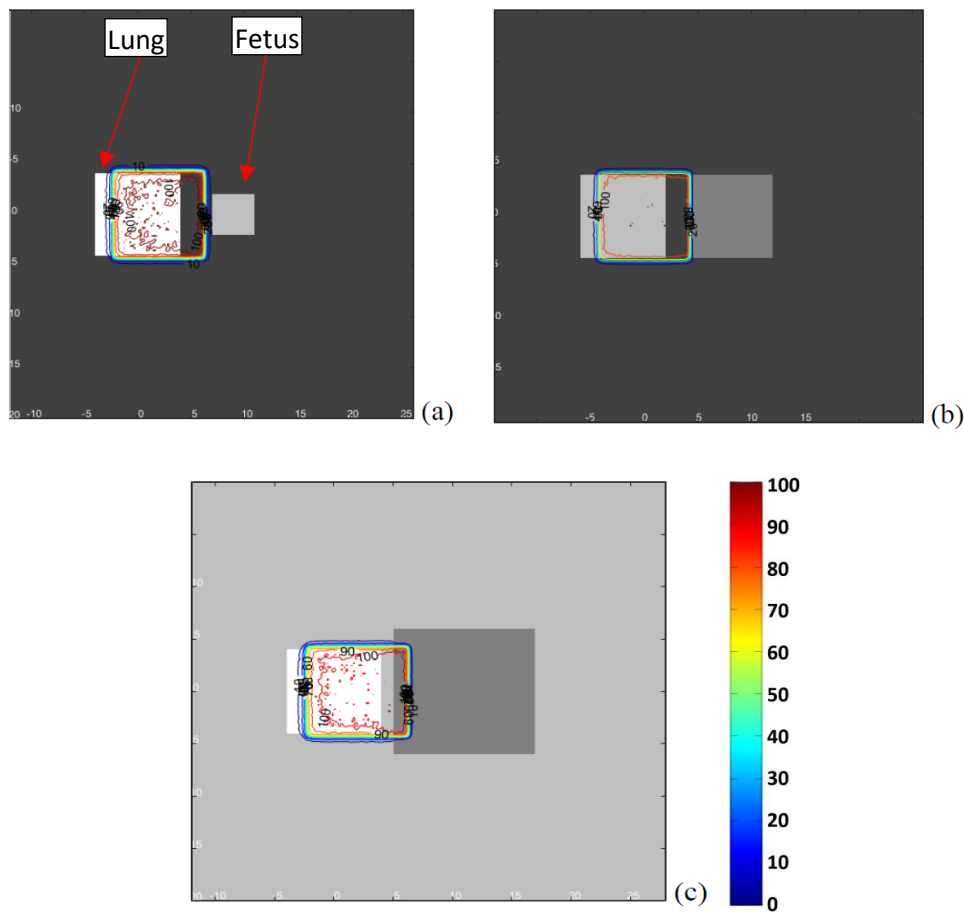


Figure 2. The isodose curve at (a) trimester 1, (b) trimester 2, and (c) Trimester 3

Figure 2 shows the isodose curves from the simulation with varying fetal ages. In Figure 2a, the fetus in the first trimester received no radiation dose. Figure 2b, which showed the fetus in the second trimester, indicated that the fetus was exposed to radiation doses ranging from 20% to 100%. However, the area receiving this dose was not as large as in the third trimester (Figure 2c), where the fetus received doses ranging from 10% to 100%.

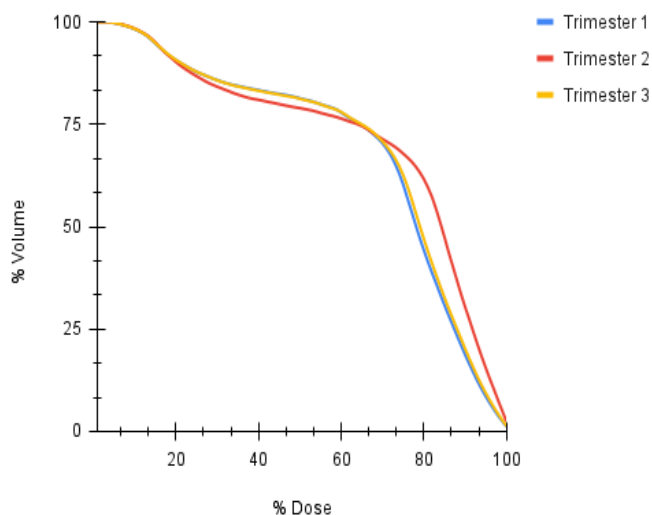


Figure 3. DVH curve of the lung with varied fetal ages

The DVH curve in Figure 3 shows the dose received by the lung. The dose received by the lung was the same for each trimester. This was because the treatment of the lung was kept consistent for each variation in fetal age. The fetus in the first trimester received a dose of 1% to 13% in 0.02% of its volume. The fetus in the second trimester also received a dose of 1% to 100% in 0.04% of its volume. The fetus in the third trimester received a dose of 1% to 100% in 0.07% of its volume. These percentages were calculated from the total volume of the fetus in each trimester.

The simulation data showed that the fetus in the first trimester received the least dose. In the second and third trimesters, the fetus received a 100% dose, but the 100% dose received by the fetus in the third trimester covered a larger area. As the fetus grew older, the dose received also increased. This was because as the fetus aged, its size increased, making it closer to the lung as the irradiation site. The fetus also received radiation doses when the lung was irradiated due to the closer proximity of the fetus to the lung. These results are in line with research conducted by Mazonakis et al. (2026) showed that an increase in fetal age resulted in an upward in fetal dose.

Photon Beam Energy

The particle source used in this study was a monoenergetic photon beam with energies of 3 MeV and 5 MeV, positioned 48 cm from the phantom. The field size was set to 8×8 cm², with irradiation location 2 being closer to a 9-month-old fetus or in the third trimester. Figure 4 showed the isodose curves for 3 MeV and 5 MeV energy variations. At 3 MeV photon energy, the fetus received a dose ranging from 10% to 100%. In Figure 4b, for 5 MeV photon energy, the fetus also received a dose within the same range. Both dose distributions indicated the same minimum and maximum doses at both energies.

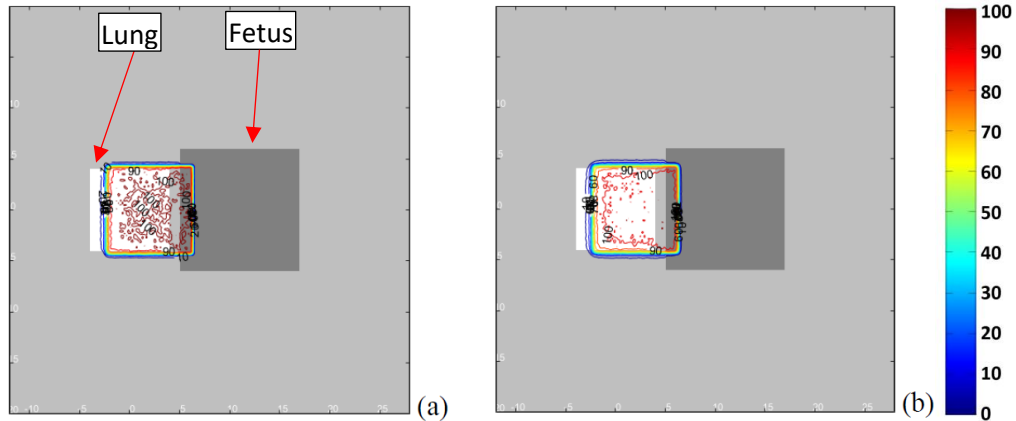


Figure 4. Isodose curve with energies of (a) 3 MeV and (b) 5 MeV

The DVH curve in Figure 5 also showed that the volume exposed to radiation had nearly the same percentage. The DVH curve in Figure 5 with energy variations showed that lung irradiated with 3 MeV energy received a lower dose than with 5 MeV energy. Radiotherapy treatment on the lung also affected the fetus. The radiotherapy simulation with 3 MeV energy gave a dose ranging from 1% to 100% to 0.03% of the fetus. Meanwhile, the fetus received a dose ranging from 1% to 100% to 0.07% of its volume. The data obtained showed that at both 3 MeV and 5 MeV energy levels, the fetus received doses up to 100%. However, at 5 MeV energy, the area of the fetus receiving up to 100% dose is larger. 5 MeV photon radiation causes the fetus to receive the maximum dose over a larger area. Additionally, the lung's dose is higher than 3 MeV photons. 5 MeV photons undergo more interactions, leading to ionization. More interactions result in more photon energy being deposited, thus increasing the absorbed dose.

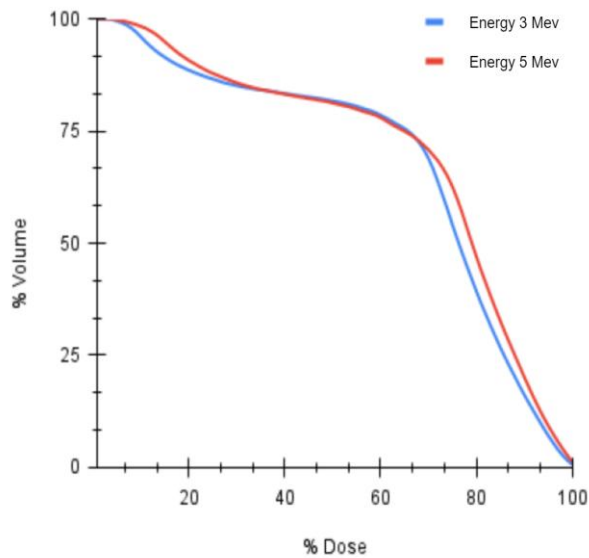


Figure 5. DVH curve of lung with energy variation

Field Size

The field size in radiotherapy indicates the area that will receive the radiotherapy treatment. The field size had to be precisely adjusted to match the size of the cancer, ensuring that only the target area was exposed to radiation while protecting the surrounding healthy tissue. This study was conducted using field sizes of $5 \times 5 \text{ cm}^2$ and $8 \times 8 \text{ cm}^2$. The fetus was set in the third trimester and irradiated with 5 MeV photon energy at irradiation beam 2. The following are the isodose and DVH curves obtained (Figures 6 and 7). A field size of $5 \times 5 \text{ cm}^2$ caused the fetus to receive a dose of 10%. In contrast, with a field size of $8 \times 8 \text{ cm}^2$, the fetus received a larger dose ranging from 10% to 100%. The resulting isodose curve illustrated that the fetus received a higher dose with the $8 \times 8 \text{ cm}^2$ field size.

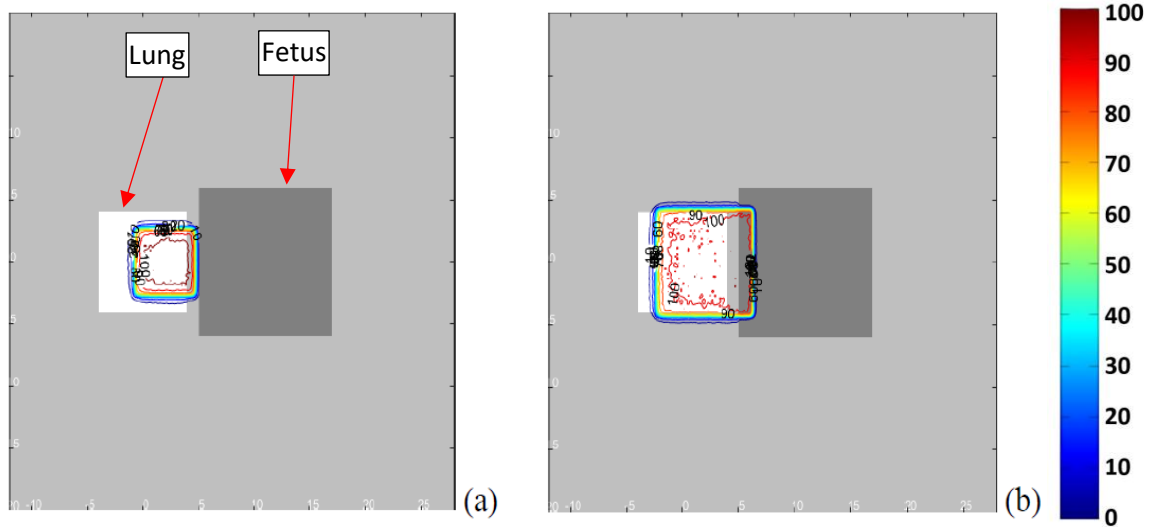


Figure 6. Isodose curves with field size (a) $5 \times 5 \text{ cm}^2$ and (b) $8 \times 8 \text{ cm}^2$

The results from the DVH curve in Figure 7 showed that the dose received by the lung with an $8 \times 8 \text{ cm}^2$ field size was higher than a $5 \times 5 \text{ cm}^2$ field size. This study focuses on the dose received by the fetus. With a $5 \times 5 \text{ cm}^2$ field size, the fetus received a dose ranging from 1% to 37% over 0.009% of its volume. In contrast, an $8 \times 8 \text{ cm}^2$ field size resulted in a dose ranging from 1% to 100% over 0.07% of the fetus's volume. Lung radiotherapy with an $8 \times 8 \text{ cm}^2$ field size resulted in the fetus receiving a higher dose compared to a $5 \times 5 \text{ cm}^2$ field size. A larger field size produced a broader dose distribution. With a larger field size, the radiation spread became less localized to the lung, allowing the radiation beam to impact the fetus.

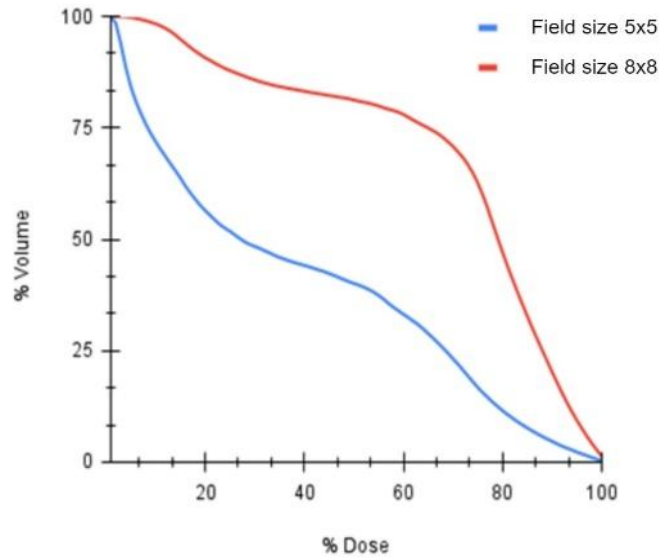


Figure 7. DVH curve of lung with field size variation

Beam Location

This study was conducted with the lung as the irradiation site, as shown in Figure 1. Irradiation location 1 was set at the center of the lung, 5 cm away from the fetus, while irradiation beam 2 was set at the lower part of the lung, 3 cm from the fetus. The fetus was set at the third trimester because, at this stage, the fetus was closer to the lung. The results included the isodose curves and DVH curves obtained.

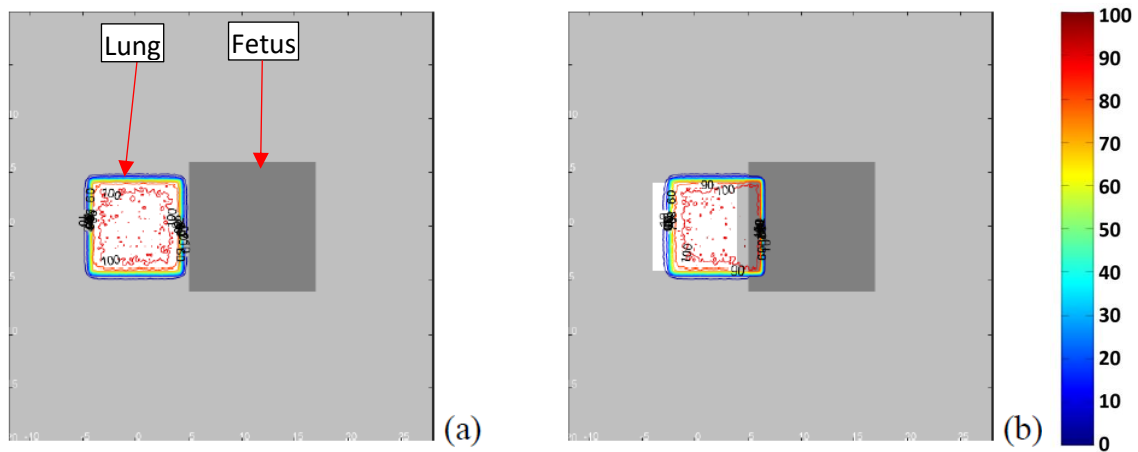


Figure 8. Isodose curves of irradiation sites in (a) beam 1 and (b) beam 2

Figure 8 show the isodose curves from the dose distribution simulation for irradiation locations 1 and 2. In Figure 8a, the irradiation location was set to beam 1, showing that the fetus did not receive any radiation at all. In contrast, Figure 8b, where the irradiation location was set to location 2, demonstrates that the fetus received doses ranging from 10% to 100%.

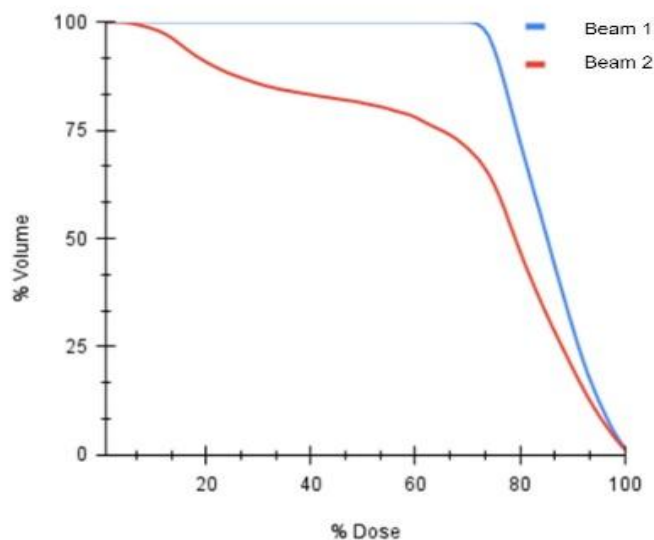


Figure 9. DVH curve of lung with variation of irradiation location

The DVH curve in Figure 9 shows that a 100% dose was achieved in a larger area of the lung at irradiation beam 1. Conversely, the fetus received a higher dose when irradiation was conducted at beam 2. This was due to the fetus being closer to the irradiation site, which resulted in the fetus being exposed to scatter from the photon beam. Irradiation at beam 1 resulted in the fetus receiving a dose ranging from 1% to 12% over 0.07% of its volume. In contrast, irradiation at beam 2 led to the fetus receiving a dose ranging from 1% to 100% over 0.075% of its volume. This demonstrates that a closer irradiation location to the fetus results in a higher dose received by the fetus.

Conclusion

This study was conducted using a $40 \times 40 \times 40$ cm³ phantom with variations in fetal age, photon beam energy, field size, and irradiation location. Simulations revealed that the fetus in the third trimester received the highest dose. This is because the fetus is larger in the third trimester, making it closer to the lung, which serves as the irradiation site. In terms of photon energy variations, it was found that higher energy levels led to higher doses received by the fetus. Greater energy causes more interactions and more energy deposition. Irradiation in beam 2, positioned at the lower part of the lung, resulted in a higher absorbed dose for the fetus due to its closer proximity to the lung as the irradiation site. The large field size also increases the dose to the fetus.

Acknowledgment

This research was funded by Dana Abadi Perguruan Tinggi-Lembaga Pengelola Dana Pendidikan (DAPT-LPDP) through national research collaboration funding program (Riset Kolaborasi Nasional) with the Grant No. 543/IT3.D10/PT.01.03/P/B/ 2023.

References

- [1] O. D. Asmara, E. D. Tenda, G. Singh, C. W. Pitoyo, C. M. Rumende, W. Rajabto, N. R. Ananda, I. Trisnawati, E. Budiyo, H.F Thahadian, E. C. Boerma, A. Faisal, D. Hutagaol, W. Soeharto, F. Radityamurti, E. Marfiani, P. Z. Romadhon, F. N. Kholis, H. Suryadinata, A. Y. Soeroto, S. A. Gondhowiardjo, W. H. Geffen, "Lung Cancer in Indonesia", *Journal of Thoracic Oncology*, vol. 18, no. 9, pp. 1134 - 1145, June. 2023.
- [2] S. H. Bradley, M. P. T. Kennedy, R. D. Neal, "Recognising Lung Cancer in Primary Care", *Adv Ther*, vol. 36, no. 1, pp. 19 - 30, 2019.
- [3] D. Palma, O Visser, F. J. Lagerwaard, J. Belderbos, B. J. Slotman, S. Senan, "Impact Of Introducing Stereotactic Lung Radiotherapy For Elderly Patients With Stage I Non-Small-Cell Lung Cancer: A Population-Based Time-Trend Analysis", *J Clin Oncol*, vol. 28, no. 35, pp. 5153-9, Dec. 2010.
- [4] E. D. Brooks, B. Sun, L. Zhao, R. Komaki, Z. Liao, M. Jeter, "Stereotactic Ablative Radiation Therapy is Highly Safe and Effective for Elderly Patients with Early-stage Non-Small Cell Lung Cancer", *Int J Radiat Oncol Biol Phys*, vol. 98, no. 4, pp. 900-907, Jul. 2017.
- [5] S. Senthil, F. J. Lagerwaard, C. J. Haasbeek, B. J. Slotman, S. Senan, "Patterns Of Disease Recurrence After Stereotactic Ablative Radiotherapy For Early Stage Non-Small-Cell Lung Cancer:A Retrospective Analysis", *Lancet Oncol*, vol. 13, no. 8, pp. 802-9. Aug. 2012.
- [6] P. Iyengar, K. Westover, R. D. Timmerman, "Stereotactic Ablative Radiotherapy (SABR) For Non-Small Cell Lung Cancer", *Semin Respir Crit Care Med*, vol. 34, no. 6, pp. 845-54, Dec. 2013.
- [7] K. Wang, J. E. Tepper, "Radiation Therapy-Associated Toxicity: Etiology, Management, And Prevention". *CA Cancer J Clin*, vol. 71, no. 5, pp. 437-454, Jul. 2021.
- [8] S. Boussios, S. N. Han, R. Fruscio, M. J. Halaska, P. B. Ottevanger, F. A. Peccatori, L. Koubkova, N. Pavlidis, F. A. Mamant, "Lung Cancer in Pregnancy: Report of Nine Cases from An International Collaborative Study", *Lung Cancer*, vol. 82, no. 3, pp. 499-505, 2013.
- [9] H. B. Kal, H. Struikmans. "Radiotherapy During Pregnancy: Fact and Fiction", *Lancet Oncol*, vol. 6, no. 5, pp. 328-333, May. 2005.
- [10] D. Pereg, G. Koren, M. Lishner, "Cancer in pregnancy: Gaps, challenges and solutions", *Cancer Treatment Reviews*, vol. 34, no. 4, pp. 302-312, Jun. 2008.
- [11] S. Y. Woo, L. M. Fuller, J. H. Cundiff, M. L. Bondy, F. B. Hagemester, P. McLaughlin, W. S. Velasquez, F. Swan, M. A. Rodriguez, F. Cabanillas, P. K. Allen, R. J. Carpenter, "Radiotherapy During Pregnancy for Clinical Stages IA-IIA Hodgkin's Disease", *Int J Radiat Oncol Biol Phys*, vol. 23, no. 2, pp. 407-412, 1992.
- [12] E. Angel, C. V. Wellnitz, M. M. Goodsitt, N. Yaghai, J. J. DeMarco, C. H. Cagnon, J. W. Sayre, D. D. Cody, D. M. Stevens, A. N. Primak, C. H. McCollough, M. F. McNitt-Gray,

- “Radiation Dose to The Fetus for Pregnant Patients Undergoing Multidetector CT Imaging: Monte Carlo Simulations Estimating Fetal Dose for A Range of Gestational Age and Patient Size”, *Radiology*, vol. 249, no. 1, pp. 220-7, Oct. 2008.
- [13] M. Mazonakis, A. Tzedakis, J. Damilakis J, “Monte Carlo Simulation of Radiotherapy for Breast Cancer in Pregnant Patients: How to Reduce the Radiation Dose and Risks to Fetus”, *Radiation Protection Dosimetry*, vol. 175, no. 1, pp. 10-16, Sep. 2016.
- [14] M. Aabid, S. Semghouli, B. Amaoui, A. Choukri. “Evaluation Of Fetal Dose During Pelvimetry CT Scan Procedure by Monte Carlo Using GATE”, *Radiation Physics and Chemistry*, vol. 210, pp. 111042, Sep. 2023.
- [15] R. Mohan, J. Antolak, “Monte Carlo Techniques Should Replace Analytical Methods for Estimating Dose Distributions in Radiotherapy Treatment Planning”, *Med. Phys*, vol. 28, no. 2, pp. 123-126, Feb. 2001.
- [16] I. F. Maulana, S. Yani, T. Sumaryada, M. F. Rhani, F. Haryanto, “Commissioning of Elekta Infinity™ 6 MV flattening filter-free using Monte Carlo simulation”, *Radiation Physics and Chemistry*, vol. 210, pp. 11101, Sep. 2023.
- [17] S. Yani, Y. A. Noviantoro, M. F. Rhani, T. Sumaryada, F. Haryanto, “Verification Of 3D-CRT Dose Distribution in Arccheck Phantom Using Monte Carlo Code”, *Radiation Physics and Chemistry*, vol. 210, pp. 111019, Sep. 2023.
- [18] M. S. Wyatt, L. F. Miller, "A comparison of Monte Carlo and model-based dose calculations in radiotherapy using MCNPTV", *Nuclear Instruments and Methods in Physics Research Section A: Accelerators, Spectrometers, Detectors and Associated Equipment*, vol. 562(2), pp. 1013-1016, 2006.
- [19] J. Park, C. Kung, "Monte Carlo Based Algorithms Are More Accurate for Dose Calculations in Radiotherapy", *Biomedical Science and Engineering*, vol. 2, no.2, pp. 40-41, 2014.
- [20] J. Wu, Y. Xie, Z. Ding, F. Li, L. Wang, "Monte Carlo study of TG-43 dosimetry parameters of GammaMed Plus high dose rate 192Ir brachytherapy source using TOPAS", *J Appl Clin Med Phys*, vol. 22, pp. 146-153, 2021.
- [21] L. Brualla, M. Rodriguez, J. Sempau, P. Andreo, “PENELOPE/PRIMO-Calculated Photon and Electron Spectra from Clinical Accelerators”, *Radiat Oncol*, vol. 14, no. 6, pp. 6, Jan. 2019.
- [22] Y. Benameur, M. Tahiri, M. Mkimel, R. E. Baydaoui, M. Najeh, S. Sahraoui, N. Benchekroun, M. Bougteb, B. E. Hariri, M. R. Mesradi, A. Hilali, E. M Saad, “Fetal Dose Estimation During Pregnancy Using Gate Monte Carlo Simulation: Application of Hodgkin’s Lymphoma Radiotherapy”, *Radiation Protection Dosimetry*, vol. 199, no. 7, pp. 581-587, May. 2023.

- [23] C. Geng, M. Moteabbed, J. Seco, Y. Gao, X. G. Xu, J. R. Méndez, B. Faddegon, H. Paganetti, "Dose Assessment for The Fetus Considering Scattered and Secondary Radiation from Photon and Proton Therapy When Treating a Brain Tumor Of The Mother", *Phy Med Biol*, vol. 61, no. 2, pp. 683, Jan. 2016.
- [24] B. Walters, I. Kawrakow, D. W. O. Rogers, "DOSXYZnrc User's Manual", *National Research Council of Canada, Ottawa, (Canada), 2023*.
- [25] I. D. Nurhadi, R. Ramdani, F. Haryanto, Y. S. Perkasa, M. Sanjaya, "Analysis of Effect of Change Source to Surface Distance (SSD) and the Field Size to Distribution Dose Using Monte Carlo Method-EGSnrc", *Indonesian Journal of Physics*, vol. 30, no. 1, pp. 14-17, Jul. 2019.
- [26] N. F. Nuzula, K. Adi, C. Anam, "Correction of 2D Isodose Curve on the Sloping Surface Using Tissue Air Ratio (TAR) Method", *Jurnal Sains dan Matematika*, vol. 23, no. 3, pp. 65-72, 2015.
- [27] R. Fardela, A. M. Putri, I. Andriani, F. Diyona, R. Analia, D. Mardiansyah, "Analysis of OAR Dose in Radiotherapy for Sinastra Breast Cancer at Universitas Andalas Hospital", *Natural Science: Jurnal Penelitian Bidang IPA dan Pendidikan IPA*, vol. 9, no. 2, pp. 112-123, Sep 2023.
- [28] D. Septhya, K. Rahayu, S. Rabbani, V. Fitria, Rahmadden, Y. Irawan, R. Hayami, "Implementation of Decision Tree Algorithm and Support Vector Machine for Lung Cancer Classification", *MALCOM: Indonesian Journal of Machine Learning and Computer Science*, vol. 3, no. 1, pp. 15-19, Apr 2023.
- [29] Z. R. Utami, Margono, Y. Kusmiyati, "Hubungan Hamil Usia Dini dengan Kejadian BBLR di Kecamatan Karangmojo Kabupaten Gunungkidul Tahun 2018", *B.S. thesis, Dept. of Midwifery, Poltekkes Kemenkes Yogyakarta, Yogyakarta, 2020*